JOURNAL OF VIROLOGY, June 1994, p. 3467–3477
0022-538X/94/$04.00+0

Vol. 68, No. 6

The Apoptotic Suppressor P35 Is Required Early during Baculovirus Replication and Is Targeted to the Cytosol of Infected Cells

PAMELA A. HERSHBERGER, DOUGLAS J. LACOUNT, AND PAUL D. FRIESEN*

Institute for Molecular Virology and Department of Biochemistry, Graduate School and College of Agricultural and Life Sciences, University of Wisconsin—Madison, Madison, Wisconsin 53706

Received 16 December 1993/Accepted 15 February 1994

The *p35* gene of *Autographa californica* nuclear polyhedrosis virus (Ac*M*NPV) is required to block virus-induced apoptosis. The *trans*-dominant activity of *p35* suppresses premature cell death and facilitates Ac*M*NPV replication in a cell line- and host-specific manner. To characterize the *p35* gene product (P35), a specific polyclonal antiserum was raised. As revealed by immunoblot analyses of wild-type Ac*M*NPV-infected cells, P35 appeared early (8 to 12 h) and accumulated through the late stages of infection (24 to 36 h). Biochemical fractionation of cells both early and late in infection and indirect immunochemical staining demonstrated that P35 localized predominantly to the cytosol (150,000 × *g* supernatant); comparatively minor quantities of P35 were associated with intracellular membranes. The cytoplasmic localization of P35 was independent of virus infection. The functional significance of the early and late synthesis of P35 was examined by constructing recombinant viruses in which the timing and level of *p35* expression were altered. Delaying P35 synthesis by placing *p35* under exclusive control of a strong, very late promoter failed to suppress intracellular DNA fragmentation and apoptotic blebbing in most cells. Thus, earlier expression of *p35* was required to block virus-induced apoptosis. Site-specific mutagenesis of the *p35* promoter demonstrated that low levels of P35 were sufficient to block apoptosis, whereas higher levels were required to maintain wild-type virus gene expression. Consistent with an early role in infection, P35 was also detected in the budded form of Ac*M*NPV. Because of the lack of sequence similarity and its cytosolic targeting, P35 may function in a manner that is mechanistically distinct from other apoptotic regulators, including Bcl-2 and the adenovirus E1B 19-kDa protein.

Productive infection of host insect cells with *Autographa californica* nuclear polyhedrosis virus (Ac*M*NPV), a prototype member of the family *Baculoviridae*, yields budded virus (BV) by plasma membrane budding and occluded virus (OV) by release from the nucleus upon cell lysis later in the replication cycle (for reviews, see references 4 and 36). In contrast, infection with Ac*M*NPV mutants lacking a functional *p35* gene causes premature cytolysis, a reduction in BV production, and nearly complete elimination of OV production (8, 18). Cell death induced by *p35* null mutants is the result of apoptosis (programmed cell death) (8), an active process characterized by the degradation of host nuclear DNA into oligonucleosome-size fragments and the disintegration of affected cells into smaller, membrane-bound vesicles (apoptotic bodies). Apoptosis can be induced by diverse stimuli, including infection by both DNA and RNA viruses (reviewed in reference 52). Baculovirus-induced apoptosis can be suppressed by infection with Ac*M*NPV that contains a wild-type copy of *p35*. Thus, *p35* functions as a *trans*-dominant regulator of virus-induced programmed cell death (8, 18). The mechanism by which *p35* suppresses apoptosis, either directly or indirectly, is unknown.

Optimum replication of Ac*M*NPV is correlated with *p35*-mediated inhibition of apoptosis that is both cell line and host specific (9, 18). Suppression of *p35* null mutant-induced apoptosis by *trans* complementation in *Spodoptera frugiperda* SF21 cultures leads to increased yields of mutant virus (18). Moreover, as demonstrated by serial passage of virus mixtures, *p35* confers a dramatic selective advantage to Ac*M*NPV by facilitating virus replication in apoptosis-sensitive cells (32). In contrast, *p35* null mutants multiply to wild-type levels in cultured *Trichoplusia ni* TN368 cells which fail to exhibit an apoptotic response (9, 18). The striking difference between the lethality of *p35* deletion mutant BV and wild-type BV when injected into larvae of *S. frugiperda* but not *T. ni* indicated that *p35* also affects virus multiplication in the host organism and suggests that this gene represents a host range determinant (9). Although it is not known whether *p35* promotes virus replication independently of its antiapoptotic activity, these findings support the general hypothesis that animal viruses, including the baculoviruses, have evolved mechanisms regulating apoptosis to facilitate replication and thereby promote their own survival (6, 8, 15–17, 33, 40).

The product of the *p35* gene (P35) is required for suppression of Ac*M*NPV-induced apoptosis (8, 18), yet little is known about this protein and its synthesis. Transcription of *p35* begins within the first hour of infection in response to host RNA polymerase II (23, 35), suggesting that P35 represents an early gene product. The *p35* promoter contains early and late regulatory motifs and is affected by the adjacent transcriptional enhancer *hr5* (Fig. 1) (11, 42). Based on nucleotide sequence and in vitro translation of *p35*-specific mRNA from infected cells (13), the predicted mass of P35 (299 amino acid residues) is 35 kDa. Truncation at amino acid residue 76 by creation of a frameshift mutation (18) or by fusion to *Escherichia coli lacZ* (8) caused loss of P35 function in Ac*M*NPV recombinants. Similarly, the lysine-rich C terminus of P35 is required for

* Corresponding author. Mailing address: Institute for Molecular Virology, Bock Laboratories, University of Wisconsin—Madison, 1525 Linden Dr., Madison, WI 53706-1596. Phone: (608) 262-7774. Fax: (608) 262-7414.

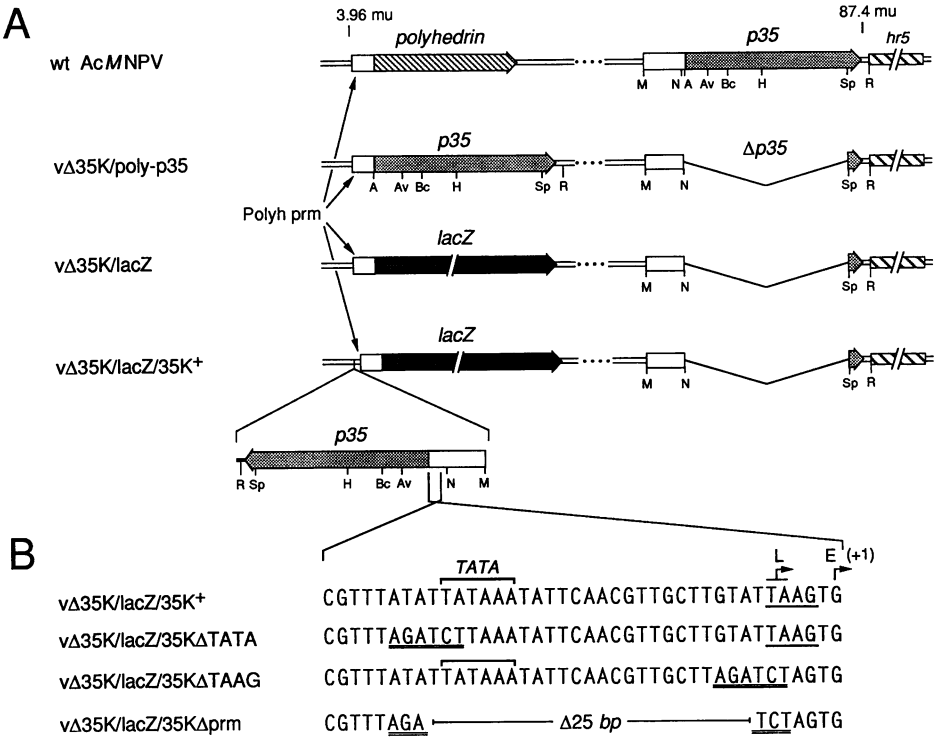

FIG. 1. Gene organization of Ac*M*NPV recombinants with altered *p35* expression. (A) Genotypes of wild-type Ac*M*NPV and recombinant viruses vΔ35K/poly-p35, vΔ35K/lacZ, and vΔ35K/lacZ/35K$^+$. Except for wild-type (wt) Ac*M*NPV, *p35* was deleted from its normal position (87.4 map units [mu]) located adjacent to the *hr5* transcriptional enhancer. The polyhedrin gene was replaced with either *p35* (light arrow) or *lacZ* (dark arrow), each under control of the polyhedrin promoter (Polyh prm). In virus vΔ35K/lacZ/35K$^+$, *p35* and its full-length promoter were inserted at the polyhedrin locus (3.96 map units). The arrows depict the direction of transcription of each gene. Abbreviations for *p35*-specific restriction sites: A, *Alu*I; Av, *Ava*II; Bc, *Bcl*I; H, *Hin*dIII; M, *Mlu*I; N, *Nru*I; R, *Eco*RI; Sp, *Spe*I. (B) Nucleotide sequences of *p35* promoter mutations. Oligonucleotide-mediated alterations were constructed within the *p35* promoter, fused to a wild-type copy of *p35*, and inserted at the polyhedrin locus next to the *lacZ* gene, thereby generating viruses with a genomic organization identical to that of vΔ35K/lacZ/35K$^+$ (A); introduced *Bgl*II sites are double underlined. The TATA element (overlined) is indicated along with the *p35* early (E) transcription start site (+1). The late (L) transcriptional start site is indicated within the consensus late TAAG motif (single underline).

protein function (18). Indicating that *p35* is highly conserved between related viruses, the Ac*M*NPV copy of *p35* exhibits 90% amino acid sequence identity to that of *Bombyx mori* nuclear polyhedrosis virus (13, 26). However, P35 bears no obvious sequence similarity with other proteins required for apoptotic suppression, including the product of the mammalian proto-oncogene *bcl-2*, adenovirus 19-kDa E1B, Epstein-Barr virus BHRF1, and the product of the granulosis virus *iap* gene (7, 10, 37, 50).

To gain insight into the molecular mechanism of *p35* function, we first examined the synthesis and intracellular localization of P35 upon Ac*M*NPV infection. By using a polyclonal antiserum, we report here that P35 is synthesized as a low-abundance, 35-kDa polypeptide that is targeted predominantly to the soluble, cytosolic compartment of infected cells. P35 appeared early (8 to 12 h) at the onset of viral DNA replication and continued to accumulate later in infection. Thus, the kinetics of P35 synthesis were consistent with an early and possibly a late function, previously suggested by the requirement for *p35* in maintaining late virus gene expression and virus DNA replication (9, 18). To examine the temporal significance of P35 synthesis, we constructed Ac*M*NPV recombinants in which the timing and level of *p35* expression were altered. Very late expression of *p35* was insufficient to prevent premature cell death and thus indicated that P35 acts earlier to block apoptosis. Only low levels of P35 were required to block host nuclear DNA fragmentation and cytolysis, although higher levels were necessary to maintain Ac*M*NPV very late gene expression. Thus, P35 may suppress virus-induced apoptosis through a catalytic mechanism or by interacting with low-abundance host death regulators.

MATERIALS AND METHODS

Cells and virus. *S. frugiperda* IPL-SF21 (45) and *T. ni* TN368 (19) cell lines were propagated in TC100 growth medium (GIBCO Laboratories) supplemented with 10% heat-inactivated fetal bovine serum (HyClone Laboratories). Wild-type Ac*M*NPV (L-1 strain) (31), wt/lacZ, vΔ35K/lacZ/35K$^+$, and *p35* deletion mutants vΔ35K and vΔ35K/lacZ were described previously (18). At time zero, monolayers were inoculated with extracellular BV. After 1 h, the residual inoculum was replaced with growth medium and the cells were incubated at 27°C. All virus titers were obtained by plaque assay using TN368 cells. In the case of *lacZ*-containing viruses, blue plaques were visualized by including 100 μg of X-Gal (5-bromo-4-chloro-3-indolyl-β-D-galactopyranoside) per ml of overlay.

Plasmid DNAs and transplacement vectors. Plasmid p35K-ORF was constructed by inserting a 1.28-kb *Mlu*I-*Eco*RI fragment, derived from the *Eco*RI S genome fragment (86.8 to 87.9 map units) of Ac*M*NPV, into the *Hin*cII and *Eco*RI sites, respectively, of the pBluescript (KS$^+$) vector (Stratagene)

containing a *Bgl*II linker at the *Xma*I site; the *Mlu*I site was end repaired with Klenow fragment prior to ligation. p35K-ORF contains the full-length promoter, the 897-bp open reading frame (ORF) of *p35*, and its polyadenylation signal. pPRM$^-$35K-ORF was constructed by inserting a 410-bp *Alu*I-*Hin*dIII fragment containing the N-terminal half of *p35* into *Eco*RV and *Hin*dIII sites, respectively, of pBluescript. The remaining portion of *p35* was added by inserting a 634-bp *Hin*dIII-*Xba*I fragment from the *Eco*RI S fragment (previously cloned into pUC19) into *Hin*dIII and *Hin*cII sites, respectively; the *Xba*I site was end repaired prior to ligation. pPRM$^-$35K-ORF contains *p35* from 15 bp upstream of the ATG codon through the downstream polyadenylation signal. pIE1^{hr}-p35 was constructed by inserting the Ac*M*NPV ie-1 promoter and *hr*5 enhancer immediately upstream from the *p35* ORF of pPRM$^-$35K-ORF (5). Transplacement plasmid pEV/35K was generated by inserting the *p35* ORF, located on a 1.1-kb *Bgl*II-*Kpn*I fragment of pPRM$^-$35K-ORF, into the corresponding sites of pEV55 (34), kindly provided by Genetics Institute (Boston, Mass.).

The *p35* promoter (Fig. 1) was mutagenized by using the oligonucleotide-mediated site-directed method of Kunkel et al. (28). Single-stranded DNA was prepared by VCSM13 helper phage (Stratagene) rescue of p35KORF-hr5$^+$, a plasmid identical to p35K-ORF except that it also contains the *hr*5 enhancer. Plasmids p35KORF-hr5$^+$ΔTATA and p35KORF-hr5$^+$ΔTAAG were obtained by using oligonucleotides 5′-GAATATTTAAGATCTAAACGTTC-3′ (positions −46 to −68 relative to the ATG codon) and 5′-GCTCACTAGATCTAAGCAACG-3′ (positions −23 to −43), respectively; *Bgl*II sites are underlined. p35KORF-hr5$^+$Δprm was constructed by inserting the 250-bp *Kpn*I-*Bgl*II promoter fragment of p35KORF-hr5$^+$ΔTATA into the corresponding sites of p35KORF-hr5$^+$ΔTAAG. Each alteration was verified by dideoxy-chain termination sequencing, and the *Nru*I-*Ava*II promoter fragments were inserted into the corresponding sites of p35K-ORF, thereby replacing the wild-type promoter. The resulting 1.28-kb *Xho*I-*Xba*I p35K-ORF fragments were inserted into the corresponding sites of the vector pEV/lacZ (18) to generate transplacement plasmids pEV/lacZ/35KΔTATA, pEV/lacZ/35KΔTAAG, and pEV/lacZ/35KΔprm.

Construction of Ac*M*NPV recombinants. Transplacement plasmid pEV/35K and parental virus vΔ35K were used in standard gene replacement procedures to generate vΔ35K/poly-p35 (Fig. 1), which was identified by its occlusion-negative plaque phenotype, using TN368 cells. To generate viruses vΔ35K/lacZ/35KΔTATA, vΔ35K/lacZ/35KΔTAAG, and vΔ35K/lacZ/35KΔprm (Fig. 1), each transplacement plasmid (10 μg) was linearized with *Not*I, mixed with ~5×10^5 PFU of vΔ35K BV, and transfected into SF21 cells by using Lipofectin (Bethesda Research Laboratories) as described previously (18). Viruses exhibiting a blue, occlusion-negative phenotype were plaque purified by using TN368 cells. The identity of each recombinant virus was established by restriction analysis of purified viral DNA. To verify the presence of the introduced mutations, the *p35* promoter-ORF fragment was amplified from virus DNA by PCR methods (2) using primers which hybridized upstream of the polyhedrin promoter and downstream within the 603 ORF. The resulting *p35*-specific DNA fragments were characterized by restriction mapping.

Antiserum and immunoblot analysis. Polyclonal rabbit antiserum was raised against a TrpE-P35 fusion protein containing P35 N-terminal amino acid residues 43 to 132. Plasmid pATH22/p35 was constructed by inserting a 269-bp *Bgl*II-*Hin*dIII *p35* fragment into the *Bam*HI and *Hin*dIII sites of pATH22 (27); the *Bgl*II site at amino acid residue 43 was introduced by mutagenesis of p35KORF-hr5$^+$, using the oligonucleotide 5′-CATGAGATCTGGTTTTGTC-3′. Insoluble protein was obtained from pATH22/p35-containing *E. coli* JM83 and subjected to preparative sodium dodecyl sulfate (SDS)-polyacrylamide gel electrophoresis. The TrpE-P35 fusion was excised, emulsified, and injected into New Zealand White rabbits (~300 μg of protein per rabbit). Anti-p35NF immune serum (α-p35NF) was collected 2 weeks after a second boost. Preimmune serum was collected prior to the first immunization. Monoclonal antibody AcV_5 to Ac*M*NPV glycoprotein gp64 (22) was a gift from Peter Faulkner (Queen's University) and kindly provided as hybridoma culture supernatant by Gary Blissard (Cornell University).

For immunoblot analyses, proteins were subjected to SDS–12.5% polyacrylamide gel electrophoresis (30) and transferred to nitrocellulose. The membranes were blocked with 5% nonfat dried milk in TBST (10 mM Tris [pH 7.4], 150 mM NaCl, 0.05% Tween 20) and incubated for 1 h at room temperature with a 1:10,000 dilution of α-p35NF or a 1:100 dilution of AcV_5 hybridoma supernatant. The membranes were then washed and incubated for 1 h with 5% nonfat dried milk–TBST containing a 1:10,000 dilution of goat anti-rabbit immunoglobulin (IgG; Pierce) or goat anti-mouse IgG (Jackson ImmunoResearch Laboratories, Inc.); both goat sera were conjugated to alkaline phosphatase. After washing with TBST, color development was initiated by incubation with 0.33 mg of nitroblue tetrazolium chloride per ml and 0.17 mg of BCIP (5-bromo-4-chloro-3′-indolylphosphate *p*-toluidine salt) per ml.

Subcellular fractionation. Infected cells were collected by low-speed centrifugation, washed twice with ice-cold phosphate-buffered saline (PBS; pH 6.2) (31), and suspended in ice-cold 10 mM Tris, (pH 7.5)–5 mM $MgCl_2$. After 5 min, the cells were subjected to Dounce homogenization (20 strokes) that provided >90% cell breakage. The nuclei were stabilized by adjusting the salt concentration to that of nuclear buffer (10 mM Tris [pH 7.5], 140 mM NaCl, 40 mM KCl, 5 mM $MgCl_2$) (2). After centrifugation (300 × *g*, 5 min), the supernatant (S1) was removed and the pelleted nuclei (N1) were washed and suspended in nuclear buffer containing 0.25 M sucrose. The nuclei were pelleted through a 1.6 M sucrose cushion for 45 min at 44,000 × *g* (SW28.1 rotor). The sucrose interface that contained nuclei without OV was collected, whereas the resulting pellet of nuclei (N2) that contained OV was suspended in nuclear buffer. Nuclear-associated membranes were solubilized by treating a portion of the N2 pellet with ice-cold 1% Triton X-100 for 30 min; the detergent-treated nuclei (N3) were collected by centrifugation (300 × *g*). The S1 fraction (see above) was adjusted to 5 mM with EDTA and subjected to centrifugation (10,000 × *g*, 10 min). The resulting heavy membrane pellet, including mitochondria, was washed with 5 mM EDTA and suspended in 10 mM Tris (pH 7.5)–140 mM NaCl–40 mM KCl. The light membranes were collected by centrifugation of the 10,000 × *g* supernatant for 1 h at 150,000 × *g* (SW41 rotor). The resulting 150,000 × *g* supernatant, containing cytosolic components, was also collected. Subcellular fractions were adjusted to 1% SDS–2.5% β-mercaptoethanol and boiled prior to analysis.

Immunolocalization. An adaptation of the method of Volkman et al. (47) was used. SF21 cells were seeded onto glass coverslips and inoculated with virus. After 48 h, the cells were washed with PHEM (pH 6.9), consisting of 60 mM PIPES [piperazine-*N*,*N*′-bis(2-ethanesulfonic acid)], 25 mM HEPES (*N*-2-hydroxyethylpiperazine-*N*′-2-ethanesulfonic acid), 10 mM EGTA, and 2 mM $MgCl_2$. The cells were fixed for 20 min with 2% paraformaldehyde in PHEM and permeabilized for 2

min with 0.5% Triton X-100–2% paraformaldehyde in PHEM. After washing with PBS (pH 7.2), the coverslips were blocked for 1 h with 3% normal donkey serum and incubated for 1 h (27°C) with a 1:500 dilution of α-p35NF or a 1:25 dilution of rabbit anti-β-galactosidase IgG (Cappel Research Products); all dilutions were made in 3% normal donkey serum and PBS. After the coverslips were incubated for 1 h with a 1:50 or 1:100 dilution of fluorescein isothiocyanate-conjugated donkey anti-rabbit IgG (Jackson ImmunoResearch), they were washed with PBS and mounted for viewing in 50 mM Tris (pH 7.8)–10% glycerol–1 mg of *p*-phenylenediamine per ml. When indicated, the primary antiserum was precleared with an acetone powder of vΔ35K-infected SF21 cells. SF21 cells (10^6 per plate) were also seeded onto glass coverslips and transfected with 2.5 μg of pIE1^{hr}-p35 by using calcium phosphate (35). After 48 h, the cells were fixed, permeabilized, and immunostained as described above. All images were obtained by using a Bio-Rad MRC-600 laser scanning confocal microscope equipped with a krypton-argon mixed-gas laser. Optical sections of 0.56 μm were obtained by using the 60× objective. Digitized images were transferred to a Macintosh Quadra 700 and prepared for presentation by Adobe Photoshop (Adobe Systems, Inc.).

BV purification. BV was collected from the growth medium of SF21 cells 48 h after infection with vΔ35K or wild-type Ac*M*NPV by centrifugation through a 25% sucrose cushion (80,000 × *g*, 75 min). Resuspended virus was subjected to centrifugation on a 20 to 70% linear sucrose gradient at 96,000 × *g* for 3 h (SW41 rotor) as described elsewhere (36). After fractionation, the BV peak was identified by applying a portion of each fraction to nitrocellulose and staining with α-gp64 AcV_5 as described above. BV was pelleted from the pooled fractions by centrifugation (80,000 × *g*, 75 min).

Internucleosomal DNA fragmentation. SF21 cells (3×10^6 per plate) were harvested 48 h after infection by low-speed centrifugation. Apoptotic vesicles were pelleted from the growth medium supernatant by centrifugation (14,000 × *g*, 15 min) at 4°C. Cells and vesicles were pooled, suspended in lysis buffer (10 mM Tris [pH 7.5], 10 mM EDTA, 0.2% Triton X-100), and extracted for low-molecular-weight DNA as previously described (24). DNA samples were treated with 0.6 mg of RNase A per ml prior to electrophoresis, using 2% agarose–Tris-borate-EDTA gels and visualization with ethidium bromide.

β-Galactosidase assays. Intracellular levels of β-galactosidase were determined as described previously (18). In brief, infected cells were harvested, washed with ice-cold PBS (pH 6.2), and suspended in 0.25 M Tris (pH 8.0). After three freeze-thaw cycles, the lysates were clarified and assayed by using the substrate *p*-nitrophenyl-β-D-galactopyranoside. When necessary, cell lysates were diluted with 0.25 M Tris (pH 8.0) to ensure linearity of the assay.

RESULTS

Identification of the apoptotic suppressor P35 and kinetics of synthesis. Our previous studies suggested that synthesis of *p35*-specific products during infection is low compared with that of other viral proteins (18). Thus, to identify and characterize *p35*-derived proteins, a polyclonal antiserum (α-p35NF) was raised against a bacterial TrpE fusion protein that contained 89 amino acids (residues 43 to 132) from a charged domain within the N-terminal half of the predicted *p35* polypeptide. Upon immunoblot analysis of total proteins from SF21 cells infected with wild-type Ac*M*NPV, α-p35NF recognized a single major polypeptide with a molecular mass of ~35 kDa (Fig. 2). The specificity of the α-p35NF was demonstrated

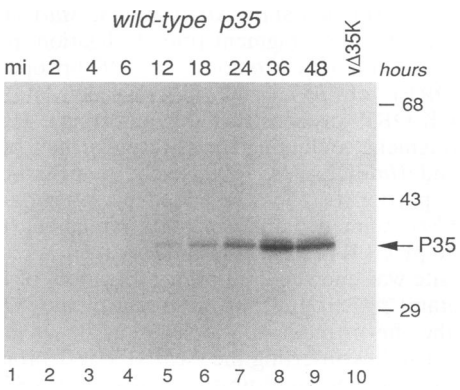

FIG. 2. Time course of P35 synthesis during wild-type Ac*M*NPV infection. SF21 cells (3×10^6 per plate) were harvested at the indicated times (hours) after infection (multiplicity of infection of 5), lysed with SDS, and subjected to SDS-polyacrylamide gel electrophoresis. Immunoblot analysis of total cellular protein (3×10^5 cell equivalents per lane) was conducted with α-p35NF. Lysates prepared from mock-infected (mi) and vΔ35K-infected cells 48 h after infection (multiplicity of infection of 5) were included. The positions of molecular weight standards (sizes in kilodaltons) and protein P35 (arrow) are indicated.

by the lack of recognition of other polypeptides in mock-infected cells or cells infected with the *p35* deletion mutant vΔ35K, as determined by immunoblotting (Fig. 2, lanes 1 and 10) and immunochemical staining of intact cells (see below). Moreover, the 35-kDa polypeptide was specifically recognized by α-p35NF when *p35* was expressed exclusively under the control of the polyhedrin promoter of recombinant vΔ35K/poly-p35 (see below) and when expressed from a *p35*-containing SP6 plasmid in reticulocyte transcription-translation extracts (29). With use of wild-type Ac*M*NPV, the 35-kDa polypeptide (hereafter designated P35) was first detected 12 h after infection and reached maximum steady-state levels by 36 h. In other analyses using *p35*-expressing Ac*M*NPV recombinants, P35 was detected by 8 h after infection (5). Less abundant species of P35 with an electrophoretic mobility slightly different from that of the predominant 35-kDa polypeptide were also detected (Fig. 2); the relative abundance of these alternate forms of P35 varied between experiments.

Intracellular localization of P35 by biochemical fractionation. To examine the subcellular distribution of P35 during wild-type Ac*M*NPV infection, SF21 cells were inoculated and homogenized both early (12 h) and later (36 h), during its maximum accumulation. Cytoplasmic and nuclear fractions were separated by using differential centrifugation. Immunoblot analysis demonstrated that a majority (>95%) of the intracellular P35 localized to the 150,000 × *g* cytosolic supernatant of cells both early (Fig. 3A, lane 2) and late (Fig. 3B, lane 2) during infection. The absence of membranes in the 150,000 × *g* supernatant was suggested by the lack of Ac*M*NPV glycoprotein gp64 in this fraction, demonstrated by using a gp64-specific monoclonal antibody (Fig. 3C, lane 2). Representing the major glycoprotein of BV, gp64 associates with intracellular and plasma membranes prior to budding (3, 46, 51) and therefore provides a useful marker for membrane proteins. As expected, gp64 localized predominantly to the heavy and light membrane fractions (Fig. 3C, lanes 3 and 4). In contrast, little P35 was detected in the heavy or light membrane fractions early (12 h) after infection, even when a 10-fold excess of each fraction was analyzed (Fig. 3A, lanes 3 and 4). Later (36 h) in infection, P35 levels increased slightly in the

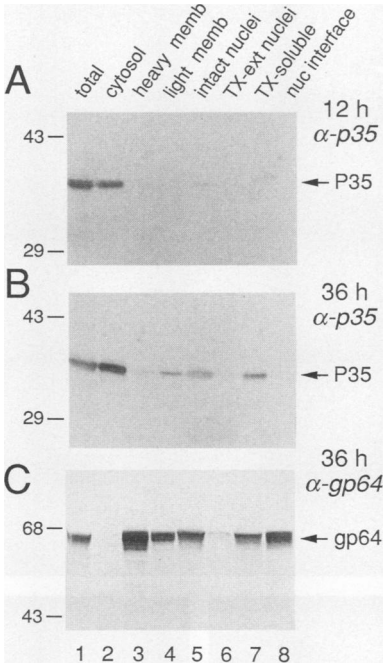

FIG. 3. Subcellular fractionation of P35 in wild-type AcMNPV-infected SF21 cells. Cells were harvested 12 and 36 h after infection (multiplicity of infection of 10) and fractionated by Dounce homogenization and differential centrifugation. The resulting fractions from cells 12 h (A) and 36 h (B and C) after infection were subjected to SDS-polyacrylamide electrophoresis and immunoblot analysis using α-p35NF (A and B) or α-gp64 monoclonal antibody AcV_5 (C). Lanes 1, total intracellular protein; 2, 150,000 × *g* cytosolic supernatant; 3, heavy membrane fraction; 4, light membrane fraction; 5, intact nuclei; 6, Triton X-100-extracted nuclei; 7, Triton X-100-soluble fraction from nuclei; 8, interface of 1.6 M sucrose cushion after sedimentation of infected cell nuclei. In panel A, each lane contains 2.5×10^5 cell equivalents, except for the heavy and light membrane fractions (lanes 3 and 4), which were increased 10-fold (2.5×10^6 cell equivalents). In panels B and C, 2.5×10^5 cell equivalents (lanes 1 and 2), 2.5×10^6 cell equivalents (lanes 3 and 4), and 5×10^5 cell equivalents (lanes 5 to 8) were used. The positions of P35, gp64, and molecular weight standards (sizes in kilodaltons) are indicated.

heavy and light membrane fractions which included mitochondria and endoplasmic reticulum, respectively (Fig. 3B, lanes 3 and 4). No P35 was detected in the nuclear interface fraction (lane 8) that contained nuclei lacking OV particles; the same nuclear interface fraction contained gp64. Minor levels of P35 were detected in the fraction (lane 5) that contained intact nuclei; at 36 h after infection, this fraction contained nuclei with OV particles. Since microscopic examination also revealed the presence of unbroken cells in the 12- and 36-h nuclear fractions, the P35 released from such cells upon SDS lysis contributed to the observed level of nuclear P35. Extraction of the intact nuclear fraction with nonionic detergent solubilized both gp64 and P35 (lane 7). This finding suggested that early and late in infection, the nuclear P35 was not tightly associated with the nucleus or it interacted with the perinuclear membrane. Biochemical fractionation (not shown) indicated a similar protein distribution when *p35* was overexpressed in cells infected with vΔ35K/poly-p35, a recombinant virus containing *p35* under control of the polyhedrin promoter (Fig. 1A).

Immunochemical staining of P35 in infected cells. The cytosolic localization of P35 was confirmed by examining the intracellular distribution of protein within intact cells. To this end, SF21 cells were fixed, subjected to indirect immunochemical staining by using α-p35NF, and viewed by fluorescent confocal laser microscopy. Infection with wild-type AcMNPV yielded a low and variable signal, which suggested that P35 was at or below the limit of detection by immunochemical staining with this serum. Intracellular P35 was therefore increased by inoculating cells with a mixture of wild-type AcMNPV and recombinant vΔ35K/poly-p35 (Fig. 1A); coinfection enhanced *p35* expression from the polyhedrin promoter and suppressed premature cytolysis caused by this virus (see below). The observed pattern of fluorescence indicated that a majority of P35 localized to the cytoplasmic compartment (Fig. 4A and B). In general, P35 was evenly distributed within the cytoplasm, although in some cells, it was concentrated nearest the plasma membrane. Little or no P35-specific fluorescence was associated with the nucleus, which was delineated by the presence of nuclear OV (polyhedra) revealed by differential-interference contrast (DIC; Nomarski) images of the same cells (Fig. 4A). SF21 cells infected with *p35* deletion mutant vΔ35K exhibited only background staining with α-p35NF (Fig. 4E); no staining was detected in intact cells or those undergoing cytolysis, as indicated by the presence of apoptotic bodies (arrows in Fig. 4E).

To determine if the intracellular distribution of P35 was dependent on virus replication, SF21 cells were transfected with plasmid $pIE1^{hr}$-p35, which directed *p35* expression in the absence of virus. Upon α-p35NF staining, transfected cells (Fig. 4C) exhibited a cytoplasmic distribution of P35 similar to that of infected cells (Fig. 4A). Thus, P35 localization was independent of viral infection. Nonetheless, comparison of these cells suggested that the accumulation of P35 in the cytoplasmic space next to the plasma membrane of infected cells (Fig. 4B) was due in part to the nuclear swelling that typically occurs during the later stages of baculovirus infection. Consistent with this effect, a dramatic concentration of β-galactosidase was also observed at the plasma membrane of cells (Fig. 4D) infected with virus wt/lacZ, in which *lacZ* expression is controlled by the polyhedrin promoter (18); β-galactosidase is a cytoplasmic protein when synthesized in these cells (25).

P35 is associated with extracellular BV. The cytoplasmic accumulation of P35 during the later stages of infection raised the possibility that it is packaged into BV, conceivably at the time when viral nucleocapsids bud from the plasma membrane. To examine this possibility, extracellular virus was purified by differential centrifugation and sucrose gradient sedimentation. As expected, immunoblot analysis demonstrated that gp64 was a major component of both wild-type BV and vΔ35K BV (Fig. 5); the lower abundance of vΔ35K gp64 was indicative of the lower yields of this virus from SF21 cells (18). Subsequent analysis using α-p35NF demonstrated that P35 was present in wild-type BV but not vΔ35K BV (Fig. 5). The electrophoretic mobility of BV-associated P35 was indistinguishable from that of intracellular P35. Compared with the major virion structural proteins gp64 and vp39 (43), however, P35 represented a minor component (data not shown). Further studies will be required to determine P35's location within enveloped BV.

Reduced P35 levels cause decreased AcMNPV very late gene expression. Besides the early appearance of P35 in infected SF21 cells, the failure of *p35* deletion mutants to initiate and/or maintain late and very late gene expression (9, 18) suggested that P35 functions early in infection. To investigate the timing and level of *p35* expression required for virus replication, we constructed a series of recombinant viruses in which P35 synthesis was altered. First, P35 accumulation was reduced by mutagenesis of the *p35* promoter (Fig. 1B). In virus vΔ35K/

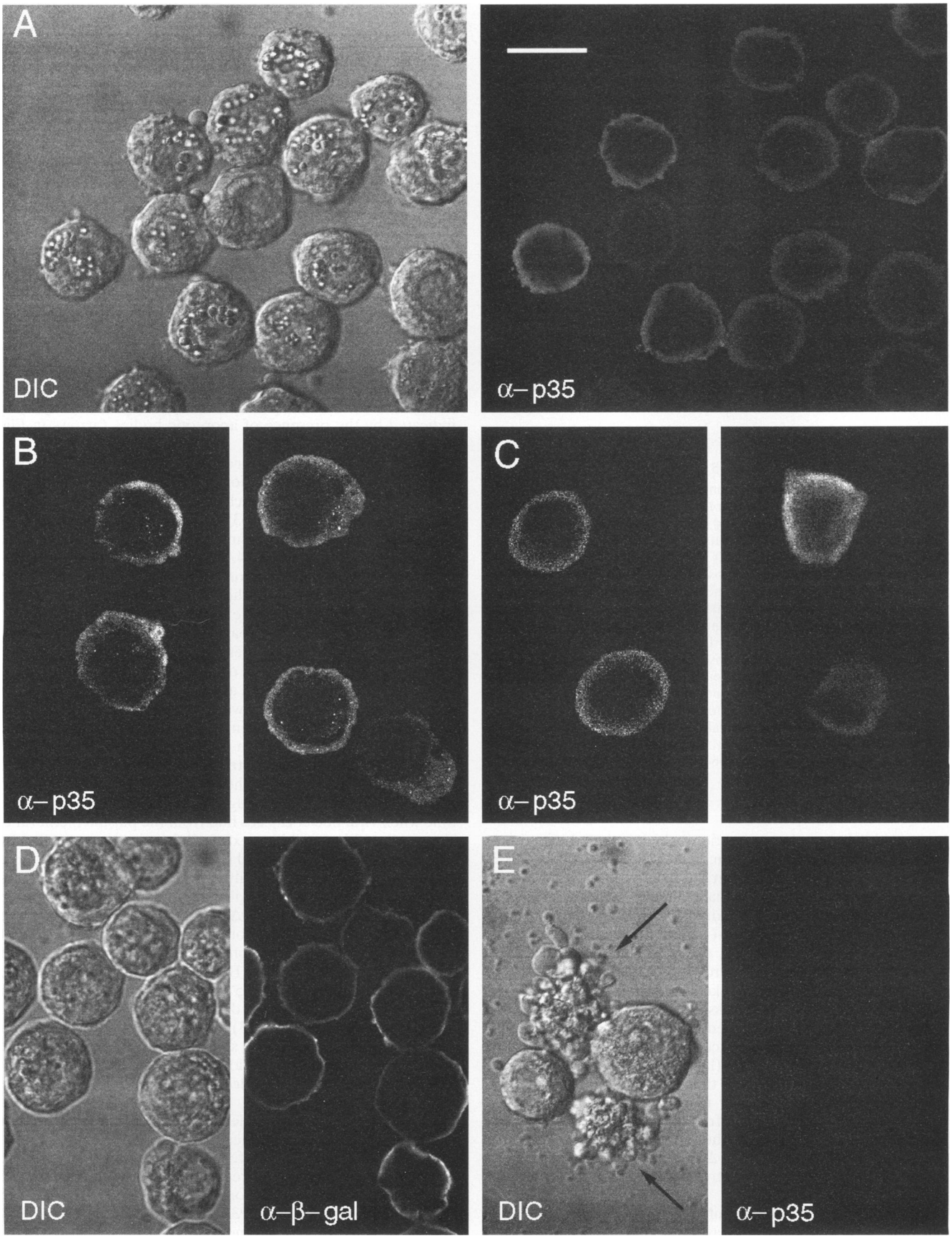
A
DIC
α–p35
B
α–p35
C
α–p35
D
DIC
α–β–gal
E
DIC
α–p35

FIG. 4. Indirect immunofluorescent localization of P35 in SF21 cells. (A) P35 immunofluorescence after coinfection with wild-type and vΔ35K/poly-p35 viruses. Coincident images by DIC (left) and fluorescent confocal laser microscopy (right) of α-p35NF (α-p35)-stained cells 48 h after infection with a 1:5 mixture of wild-type virus and vΔ35K/poly-p35, respectively, are shown. (B) Cytoplasmic distribution of P35 in AcMNPV-infected cells. Two fields of SF21 cells are shown after infection as described for panel A and staining with α-p35NF; panels A and B represent independent experiments. (C) Cytoplasmic distribution of P35 in plasmid-transfected cells. Two fields of α-p35NF-stained SF21 cells are shown 48 h after transfection with plasmid pIE1^{hr}-p35; approximately 1 to 5% of the cells exhibited P35-specific immunofluorescence. (D) β-Galactosidase distribution after infection with AcMNPV recombinant wt/lacZ. DIC (left) and fluorescence (right) images of SF21 cells 48 h after infection wt/lacZ and stained with α-β-galactosidase (α-β-gal) serum are shown. (E) Background immunofluorescence after infection with *p35* deletion mutant vΔ35K. DIC (left) and fluorescence (right) images of α-p35NF-stained SF21 cells 48 h after infection with vΔ35K are shown. The arrows depict apoptotic bodies. For all images, the cells were fixed, treated with detergent, and stained with preadsorbed primary antiserum followed by secondary fluorescein isothiocyanate-conjugated antibodies. The bar represents 20 μm.

lacZ/35KΔTATA, the TATA element was replaced, thereby decreasing early promoter activity to ~5% of that of the wild-type promoter (11). In virus vΔ35K/lacZ/35KΔTAAG, the late promoter motif TAAG (positions −2 to −5 relative to the early RNA start, +1) was replaced; elimination of the consensus late motif (ATAAG) abolishes AcMNPV transcription from this site (39, 42). Lastly, both motifs were simultaneously deleted from the promoter in virus vΔ35K/lacZ/35KΔprm.

Immunoblot analysis of total protein from infected cells demonstrated that P35 accumulation was indeed reduced by promoter mutagenesis (Fig. 6). Loss of the TATA element reduced early (12 h) P35 below the limit of detection (lane 3), whereas loss of the TAAG motif reduced P35 approximately fivefold (lane 4) compared with that synthesized at the same time by vΔ35K/lacZ/35K$^+$ with a wild-type *p35* promoter (lane 1). The reduction in P35 was most evident early in infection, since by 36 h, the level of P35 in vΔ35K/lacZ/35KΔTATA- and vΔ35K/lacZ/35KΔTAAG-infected cells was only slightly lower than that of vΔ35K/lacZ/35K$^+$-infected cells.

To determine the effect of reduced P35 levels on very late viral expression, we measured *lacZ* expression under control of the very late polyhedrin promoter in both SF21 and TN368 cultures after infection with each *p35* promoter mutant. Since polyhedrin promoter activity in TN368 cells is not affected by *p35* (18), the calculated SF21/TN368 ratio of accumulated β-galactosidase provided a means to compare the levels of gene expression for each virus (Fig. 7). Consistent with earlier studies, TN368 cells produced approximately twofold more β-galactosidase than SF21 cells (SF21/TN368 ratio of 0.44) when normal levels of P35 were synthesized from the wild-type *p35* promoter of virus vΔ35K/lacZ/35K$^+$. In contrast, β-galactosidase synthesis in SF21 cells infected with promoter mutants vΔ35K/lacZ/35KΔTATA and vΔ35K/lacZ/35KΔTAAG was significantly reduced, resulting in levels that were 39 and 25% of that of produced by vΔ35K/lacZ/35K$^+$ (100%). As expected, mutants vΔ35K/lacZ/35KΔprm and vΔ35K/lacZ synthesized even less β-galactosidase, producing only 4 and 1%, respectively, of that of vΔ35K/lacZ/35K$^+$ (Fig. 7). Thus, reduced P35 levels were correlated with decreased levels of very late gene expression that was specific to apoptosis-sensitive cells. Since the reduction in P35 was most pronounced early (12 h) in infection, these results suggested that early P35 synthesis is required for wild-type levels of gene expression.

Effects of reduced P35 synthesis on suppression of AcMNPV-induced apoptosis. To examine the level of P35 required to block apoptosis, we tested each viral recombinant for the capacity to suppress intracellular DNA degradation and apoptotic cytolysis of SF21 cells. Of the three *p35* promoter mutants, only vΔ35K/lacZ/35KΔprm failed to block intracellular DNA fragmentation into oligonucleosome-size fragments (Fig. 8). By 48 h, approximately 50 to 75% of the cells within Δ35K/lacZ/35KΔprm-infected cultures were eliminated by apoptotic blebbing, compared with nearly all cells infected with *p35* deletion mutant vΔ35K/lacZ (data not shown). As ex-

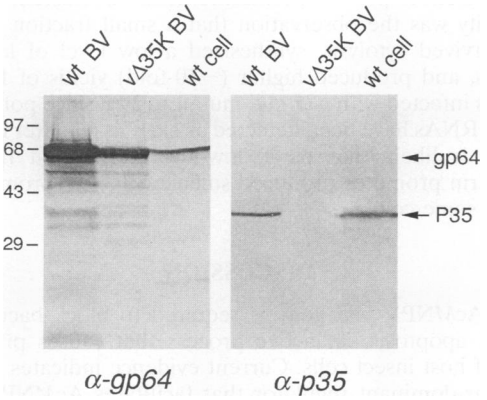

FIG. 5. Association of P35 with wild-type BV. Extracellular wild-type (wt) BV or *p35* deletion mutant (vΔ35K) BV was purified by sucrose gradient sedimentation from the growth medium of SF21 cells 48 h after infection. The BV was boiled in 1% SDS–2.5% β-mercaptoethanol, and duplicate samples were subjected to electrophoresis on an SDS–12.5% polyacrylamide gel. After transfer to nitrocellulose, the duplicate membranes were stained with α-gp64 AcV_5 or α-p35NF, respectively. Total protein lysates from wild-type AcMNPV-infected SF21 cells (wt cell) were included; positions of gp64, P35, and molecular weight standards (sizes in kilodaltons) are shown.

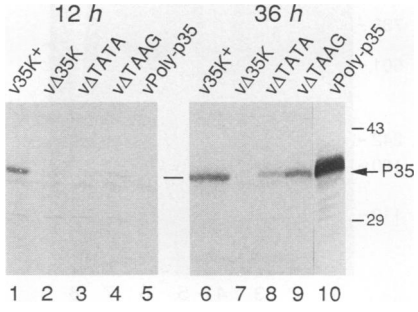

FIG. 6. Comparison of intracellular levels of P35 after infection with AcMNPV *p35* promoter mutants. SF21 cells (10^6 cells per plate) were harvested 12 and 36 h after infection (multiplicity of infection of 5) with recombinant viruses vΔ35K/lacZ/35K$^+$ (v35K$^+$), vΔ35K/lacZ (vΔ35K), vΔ35K/lacZ/35KΔTATA (vΔTATA), vΔ35K/lacZ/35KΔTAAG (vΔTAAG), and vΔ35K/poly-p35 (vPoly-p35). Immunoblot analysis of total cellular protein (3×10^5 cell equivalents per lane) was conducted with α-p35NF. Positions of molecular weight standards (sizes in kilodaltons) and P35 are indicated. To preserve sample purity, lanes 9 and 10 were separated during electrophoresis on the same gel and then spliced together after immunoblot analysis.

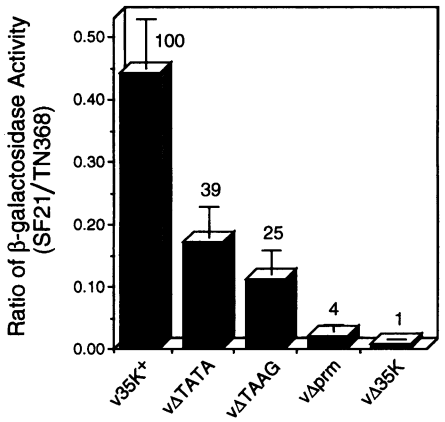

FIG. 7. Effect of altered *p35* expression on very late gene expression. SF21 and TN368 cells (10^6 per plate) were inoculated (multiplicity of infection of 5) with viruses vΔ35K/lacZ/35K$^+$ (v35K$^+$), vΔ35K/lacZ/35KΔTATA (vΔTATA), vΔ35K/lacZ/35KΔTAAG (vΔTAAG), vΔ35K/lacZ/35KΔprm (vΔprm), and vΔ35K/lacZ (vΔ35K), harvested 48 h later, and assayed for intracellular β-galactosidase. The ratio of β-galactosidase activity in SF21 to TN368 cells was calculated. The values shown represent the averages of three infections with each virus, including at least two independent isolates of vΔ35K/lacZ/35KΔTATA, vΔ35K/lacZ/35KΔTAAG, and vΔ35K/lacZ/35KΔprm; error bars are indicated. The percent reduction in the ratio of β-galactosidase compared with that determined for vΔ35K/lacZ/35K$^+$ (100%) is indicated for each viral mutant.

pected, vΔ35K/lacZ also caused extensive intracellular DNA fragmentation (Fig. 8, lane 4), whereas no fragmentation was detected in mock-infected cells or cells infected with vΔ35K/lacZ/35K$^+$ which contained *p35* under control of its own promoter (lanes 2 and 3). Despite the reduction in P35 levels, neither vΔ35K/lacZ/35KΔTATA nor vΔ35K/lacZ/35KΔTAAG induced apoptosis to the extent that DNA fragmentation was detected (lanes 5 and 6). Thus, independent loss of the TATA or TAAG motif failed to reduce P35 below the level required to block apoptosis. Since a low but reproducible level of cytolysis was observed in cultures infected with vΔ35K/lacZ/35KΔTATA but not with vΔ35K/lacZ/35KΔTAAG, the low level of P35 synthesized by the TATA mutant was at or near the threshold required for apoptotic suppression.

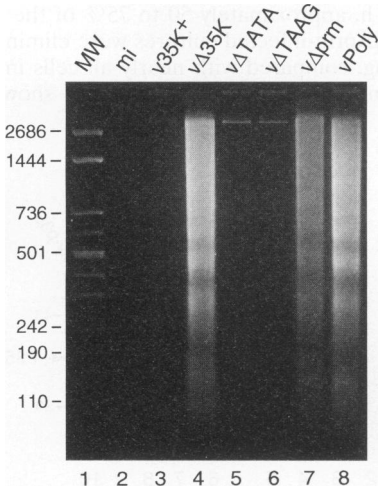

FIG. 8. Effect of Ac*M*NPV *p35* promoter mutants on suppression of intracellular DNA fragmentation. SF21 cells were inoculated (multiplicity of infection of 3) with recombinant viruses vΔ35K/lacZ/35K$^+$ (v35K$^+$), vΔ35K/lacZ (vΔ35K), vΔ35K/lacZ/35KΔTATA (vΔTATA), vΔ35K/lacZ/35KΔTAAG (vΔTAAG), vΔ35K/lacZ/35KΔprm (vΔprm), and vΔ35K/poly-p35 (vPoly). Low-molecular-weight DNA was extracted from intact cells and associated apoptotic bodies 48 h after infection and subjected to agarose gel electrophoresis (3×10^6 cell equivalents per lane). DNA from mock-infected cells (mi) was included. Positions of DNA molecular weight (MW) markers (sizes in base pairs) are indicated.

Late expression of *p35* is insufficient to block Ac*M*NPV-induced apoptosis. To further examine the requirement for early synthesis of P35, the effect of delaying *p35* expression until late in infection was examined by using vΔ35K/poly-p35. In this viral recombinant, *p35* was removed from its normal position and placed under exclusive control of the very late polyhedrin promoter (Fig. 1A). Analysis of the kinetics of protein synthesis in nonapoptotic TN368 cells verified that vΔ35K/poly-p35 replication was normal and that P35 was synthesized maximally at the times (24 to 48 h) characteristic of very late gene expression (data not shown). In contrast, vΔ35K/poly-p35 infection of SF21 cultures induced apoptosis in most cells, as demonstrated by high-level degradation of intracellular DNA into oligonucleosome-size fragments (Fig. 8, lane 8). The extent and pattern of DNA fragmentation were indistinguishable from those caused by mutant vΔ35K (lane 4). In addition, premature cytolysis and apoptotic body formation were extensive, affecting more than 50% of the cells 48 h after infection with vΔ35K/poly-p35.

Immunoblot analysis demonstrated that P35 was synthesized in SF21 cultures infected with vΔ35K/poly-p35, but only late in infection (Fig. 6). At 12 h, when P35 was readily detected in vΔ35K/lacZ/35K$^+$-infected cells (lane 1), it was below the limit of detection in vΔ35K/poly-p35-infected cells (lane 5). By 36 h, however, the vΔ35K/poly-p35 level of P35 (lane 10) exceeded that of vΔ35K/lacZ/35K$^+$ (lane 6). Thus, although the average level of P35 was higher late in infection, such expression from vΔ35K/poly-p35 was not sufficient to block apoptosis in all cells. Since very late gene expression by *p35* null mutants is typically reduced, the late appearance of P35 suggested that at least in some vΔ35K/poly-p35-infected cells, *p35* expression was sufficient to prevent premature death. Consistent with this possibility was the observation that a small fraction of these cells survived cytolysis, synthesized a low level of late virus proteins, and produced higher (~10-fold) yields of BV than did cells infected with *p35* null mutants (29). Since polyhedrin-specific RNAs have been detected as early as 6 h after infection (12), it is likely that early, low-level expression from the polyhedrin promoter produced sufficient P35 to promote survival of some cells.

DISCUSSION

The Ac*M*NPV *p35* gene is required to block baculovirus-induced apoptosis, an active process that causes premature death of host insect cells. Current evidence indicates that *p35* is a *trans*-dominant regulator that facilitates Ac*M*NPV replication and provides a selective advantage in apoptosis-sensitive cells (8, 9, 18, 32). Upon stable transfection, *p35* also inhibits apoptotic death of mammalian neural cells in a manner that resembles protection provided by overexpression of the apoptotic suppressor *bcl-2* (38, 53). In addition, *p35* expression prevents developmental programmed cell death in transgenic nematodes (*Caenorhabditis elegans*) by a mechanism that is independent of *ced-9* (44), an invertebrate regulator of cell death that bears sequence similarity to *bcl-2*. Collectively, these

findings indicate that *p35* is a general suppressor of programmed cell death in a pathway that is highly conserved among diverse organisms. Thus, it is likely that during baculovirus infection, *p35* blocks apoptosis directly by a mechanism that does not require other virus-encoded apoptotic regulators. The studies reported here investigate this mechanism by characterizing the *p35* gene product, P35.

Identification of P35 during infection. Consistent with the transcription of its gene (23, 35), P35 was detected early (8 to 12 h) in the Ac*M*NPV infection cycle. Thus, P35 was present prior to the first morphological signs of virus-induced apoptosis, including membrane blebbing beginning in some cells as early as 12 h after infection with *p35* null mutants (reference 8 and our observations). Identical early synthesis of a P35–β-galactosidase fusion protein was directed by *p35* deletion virus v35K-lacZ (18), in which the *p35* promoter directed expression of a nonfunctional *p35-lacZ* hybrid prior to apoptotic cytolysis (29). This finding suggested that even though apoptosis is initiated (see below), the *p35* promoter is capable of directing sufficient *p35* expression to counter the host response and thereby block premature death. In wild-type Ac*M*NPV-infected cells, P35 continued to accumulate late into infection, reaching maximum levels from 24 to 36 h. Nonetheless, P35 represented a low-abundance protein compared with viral structural proteins. Immunoblot analysis provided no evidence that P35 undergoes proteolytic processing, and preliminary studies have indicated that P35 is relatively stable in infected cells (5). The presence of less abundant forms of P35 with slightly altered electrophoretic mobilities suggested that P35 undergoes limited posttranslational processing. However, the type and significance of this apparent protein processing are unknown.

Apoptotic suppression by cytosolic P35. Our results indicate that P35 exists predominantly as a soluble component of the cytosol of infected cells. A majority of the P35 both early and late during infection was concentrated in the 150,000 × *g* cytosolic supernatant. Minor amounts of P35 were found in the most dense nuclear fraction; this P35 was solubilized by nonionic detergent, suggesting a weak association with the nucleus or nuclear membranes. In contrast, little, if any, P35 was detected in the heavy and light membrane fractions that included mitochondria and the endoplasmic reticulum (Fig. 3). Low-affinity interactions with intracellular membranes have not been ruled out, since our fractionation methods may have disrupted such associations. Nonetheless, the cytosolic distribution of P35 was independently confirmed by immunochemical staining of infected cells and cells transfected with a *p35*-expressing plasmid (Fig. 4).

The cytosolic localization of P35 distinguishes it from the apoptotic suppressors Bcl-2 (1, 20, 21) and adenovirus 19-kDa E1B (48, 49), which localize to membranes of the mitochondrion, endoplasmic reticula, or nucleus. When overexpressed in *S. frugiperda* SF9 cells by a baculovirus vector, Bcl-2 maintained its membrane association and exhibited little, if any, cytosolic localization (1). It has been proposed that Bcl-2's capacity to block oxidative death explains its association with these membranes, since these are the sites for generation of oxygen free radicals (21). Assuming that P35 functions at the site of highest concentration, our results suggest that apoptosis can also be suppressed by a soluble component of the cytosol. Because of the low level of P35 required to block virus-induced apoptosis, the possibility that P35 regulates cell death at a yet undefined site has not been ruled out. Nonetheless, the cytosolic targeting of P35, in addition to its apparent lack of sequence similarities with known suppressors of programmed cell death, suggests that P35 regulates apoptosis by using a distinct molecular mechanism.

Early *p35* expression is required to block Ac*M*NPV-induced apoptosis. By delaying *p35* expression, it was demonstrated that very late virus-directed synthesis alone was not sufficient to prevent apoptotic death of most cells; SF21 DNA fragmentation and apoptotic cytolysis were extensive when *p35* was placed under exclusive control of the very late polyhedrin promoter of virus vΔ35K/poly-p35 (Fig. 8). The higher synthesis of P35 in the apoptotic cells infected with this virus (Fig. 6) did not by itself cause apoptosis, since coinfection with wild-type virus resulted in its complete suppression and even greater accumulation of P35. Thus, earlier synthesis of P35 was required to suppress Ac*M*NPV-induced apoptosis. Promoter mutagenesis which caused as much as a fivefold reduction in early P35 levels had little or no effect on the virus's capacity to suppress intracellular DNA fragmentation (Fig. 8). Thus, P35 functions at low levels early in infection. This conclusion is consistent with the finding of Crook et al. (10) that early viral expression of *p35* (occurring from 0 to 5 h after infection) was sufficient to block apoptosis of SF21 cells caused by the addition of actinomycin D (1 μg/ml); it is unknown whether apoptosis induced by this transcriptional inhibitor is mechanistically similar to that induced by Ac*M*NPV. The observation that low intracellular levels of P35 are sufficient to block apoptosis suggests that this suppressor functions by using a catalytic mechanism or, alternatively, by interacting with other low-abundance death regulators present in the host cell.

Although a variety of RNA and DNA viruses have the capacity to induce apoptosis, the molecular mechanisms involved are unknown (reviewed in reference 52). In the case of Ac*M*NPV, which uses early, late, and very late replicative phases, the apoptotic signal appears to be induced in part by early viral events. This is suggested by the appearance of apoptotic manifestations (DNA fragmentation and membrane blebbing) from 6 to 12 h after infection as well as the early requirement for P35 synthesis. Apoptotic signaling could be induced by viral interactions with cellular receptors, the potential activity of early Ac*M*NPV transactivators analogous to adenovirus E1A, which induces apoptosis (40), or metabolic imbalances resulting from viral biosynthetic processes, including free-radical generation. Crook et al. (10) have correlated the beginning of Ac*M*NPV-induced apoptosis with the reduction in host RNA and protein synthesis occurring from 9 to 12 h after infection, also suggesting that virus-induced imbalances in host apoptotic regulators may be involved.

Differential requirements for P35 during Ac*M*NPV replication. The observed reduction in late gene expression and DNA replication by *p35* null mutants suggested that *p35* also functions early in infection to maintain or accelerate virus replication (9, 18). However, it was unknown whether *p35* promotes virus replication independently of its antiapoptotic activity. We have shown here that *p35* promoter mutants which exhibited a preferential reduction in early accumulation of P35 were also impaired for very late gene expression, as indicated by a 60 to 75% reduction in polyhedrin promoter-directed synthesis of β-galactosidase (Fig. 7). In contrast, the altered levels of P35 had little or no effect on suppression of apoptosis by these mutants (Fig. 8). Thus, although low levels of P35 were sufficient to block intracellular DNA fragmentation and cytolysis, higher levels were required to maintain wild-type virus gene expression and replication. Since late and very late gene expression is dependent on viral DNA replication (14, 41), incomplete suppression of apoptotic nuclease activities may reduce late gene transcription by nicking viral genomic DNA without causing extensive intracellular DNA fragmentation

and cytolysis. Thus, P35 may be indirectly required for late and very late gene expression by protecting virus DNA from apoptosis-induced nucleolytic activities. The higher levels of P35 accumulation late in infection (Fig. 2) may provide extended protection from apoptosis which occurs asynchronously in SF21 cultures, beginning from 12 h and continuing through 36 h in different cells. Alternatively, P35 may directly influence late gene expression by providing DNA replication or transactivation functions. Such viral functions must be cell line specific, since multiplication of *p35* null mutants is indistinguishable from that of wild-type virus in certain cell lines, including TN368 used in this study (9, 18).

Potential roles for P35 associated with infectious virus. Immunoblot analysis revealed that P35 copurified with wild-type BV particles of Ac*M*NPV (Fig. 5). This finding suggested that P35 is packaged within BV and that it may play a role in infection when presented to the cell in this manner. Our previous studies suggested that the progeny of *p35* deletion mutants are defective for initiating infection, since plaquing efficiencies were reduced and higher input multiplicities were required to elicit cytopathic effects compared with wild-type virus (18). Thus, virion-associated P35 may affect virus stability, attachment, or penetration of SF21 cells. Alternatively, P35 delivered to the cell by the virion may promote virus infectivity by boosting the level of this protein early in infection. Since low levels of P35 are sufficient to block apoptosis, virion-contributed P35 may provide additional protection of virus DNA from apoptotic nucleases immediately after nucleocapsid uncoating. Since *p35* also accelerates the expression of other virus genes either directly or indirectly (9, 18), increased levels of early P35 may further expedite virus replication. Additional studies will be required to determine the exact location of P35 within the BV particle and to examine its functional significance.

ACKNOWLEDGMENTS

We thank Jennifer Cartier and Julie Dickson for construction of several plasmids and recombinant viruses used in this study and Patricia Seward for initial preparation of α-p35 serum. We also thank Vicki Froehlich for assistance and advice concerning confocal laser microscopy. We thank Peter Faulkner and Gary Blissard for the gift of monoclonal antiserum AcV_5.

Microscopy support was provided in part by the Integrated Microscopy Center, U.W.—Madison, through NIH Biomedical Research Technology grant RR 00570. This work was supported in part by Public Health Service grant AI25557 from the National Institute of Allergy and Infectious Diseases and a U. W. Steenbock Career Development Award (P.D.F.).

REFERENCES

1. **Alnemri, E. S., N. M. Robertson, T. F. Fernandes, C. M. Croce, and G. Litwack.** 1992. Overexpressed full-length human BCL2 extends the survival of baculovirus-infected Sf9 insect cells. Proc. Natl. Acad. Sci. USA **89:**7295–7299.
2. **Ausubel, F. M., R. Brent, R. E. Kingston, D. D. Moore, J. G. Seidman, J. A. Smith, and K. Struhl (ed.).** 1989. Current protocols in molecular biology. John Wiley & Sons, Inc., New York.
3. **Blissard, G. W., and G. F. Rohrmann.** 1989. Location, sequence, transcriptional mapping, and temporal expression of the gp64 envelope glycoprotein gene of *Orgyia pseudotsugata* multicapsid nuclear polyhedrosis virus. Virology **170:**1–8.
4. **Blissard, G. W., and G. F. Rohrmann.** 1990. Baculovirus diversity and molecular biology. Annu. Rev. Entomol. **35:**127–155.
5. **Cartier, J. L., and P. D. Friesen.** Unpublished data.
6. **Chou, J., and B. Roizman.** 1992. The $\gamma_1$34.5 gene of herpes simplex virus 1 precludes neuroblastoma cells from triggering total shutoff of protein synthesis characteristic of programmed cell death in neurons. Proc. Natl. Acad. Sci. USA **89:**3266–3270.
7. **Cleary, M. L., S. D. Smith, and J. Sklar.** 1986. Cloning and structural analysis of cDNAs for *bcl*-2 and a hybrid *bcl*-2/immunoglobulin transcript resulting from the t(14;18) translocation. Cell **47:**19–28.
8. **Clem, R. J., M. Fechheimer, and L. K. Miller.** 1991. Prevention of apoptosis by a baculovirus gene during infection of insect cells. Science **254:**1388–1390.
9. **Clem, R. J., and L. K. Miller.** 1993. Apoptosis reduces both the in vitro replication and in vivo infectivity of a baculovirus. J. Virol. **67:**3730–3738.
10. **Crook, N. E., R. J. Clem, and L. K. Miller.** 1993. An apoptosis-inhibiting baculovirus gene with a zinc finger-like motif. J. Virol. **67:**2168–2174.
11. **Dickson, J. A., and P. D. Friesen.** 1991. Identification of upstream promoter elements mediating early transcription from the 35,000-molecular-weight protein gene of *Autographa californica* nuclear polyhedrosis virus. J. Virol. **65:**4006–4016.
12. **Friesen, P. D., and L. K. Miller.** 1985. Temporal regulation of baculovirus RNA: overlapping early and late transcripts. J. Virol. **54:**392–400.
13. **Friesen, P. D., and L. K. Miller.** 1987. Divergent transcription of early 35- and 94-kilodalton protein genes encoded by the *Hin*dIII-K genome fragment of the baculovirus *Autographa californica* nuclear polyhedrosis virus. J. Virol. **61:**2264–2272.
14. **Gordon, J. D., and E. B. Carstens.** 1984. Phenotypic characterization and physical mapping of a temperature-sensitive mutant of *Autographa californica* nuclear polyhedrosis virus defective in DNA synthesis. Virology **138:**69–81.
15. **Gregory, C. D., C. Dive, S. Henderson, C. A. Smith, G. T. Williams, J. Gordon, and A. B. Rickinson.** 1991. Activation of Epstein-Barr virus latent genes protects human B cells from death by apoptosis. Nature (London) **349:**612–614.
16. **Henderson, S., D. Huen, M. Rowe, C. Dawson, G. Johnson, and A. Rickinson.** 1993. Epstein-Barr virus-coded BHRF1 protein, a viral homologue of Bcl-2, protects human B cells from programmed cell death. Proc. Natl. Acad. Sci. USA **90:**8479–8483.
17. **Henderson, S., M. Rowe, C. Gregory, D. Croom-Carter, F. Wang, R. Longnecker, E. Kieff, and A. Rickinson.** 1991. Induction of *bcl*-2 expression by Epstein-Barr virus latent membrane protein 1 protects infected B cells from programmed cell death. Cell **65:** 1107–1115.
18. **Hershberger, P. A., J. A. Dickson, and P. D. Friesen.** 1992. Site-specific mutagenesis of the 35-kilodalton protein gene encoded by *Autographa californica* nuclear polyhedrosis virus: cell line-specific effects on virus replication. J. Virol. **66:**5525–5533.
19. **Hink, W. F.** 1970. Established insect cell line from cabbage looper, *Trichoplusia ni*. Nature (London) **225:**466–467.
20. **Hockenbery, D., G. Nuñez, C. Milliman, R. D. Schreiber, and S. J. Korsmeyer.** 1990. Bcl-2 is an inner mitochondrial membrane protein that blocks programmed cell death. Nature (London) **348:**334–336.
21. **Hockenbery, D. M., Z. N. Oltvai, X. Yin, C. L. Milliman, and S. J. Korsmeyer.** 1993. Bcl-2 functions in an antioxidant pathway to prevent apoptosis. Cell **75:**241–251.
22. **Hohmann, A. W., and P. Faulkner.** 1983. Monoclonal antibodies to baculovirus structural proteins: determination of specificities by Western blot analysis. Virology **125:**432–444.
23. **Huh, N. E., and R. F. Weaver.** 1990. Identifying the RNA polymerases that synthesize specific transcripts of the *Autographa californica* nuclear polyhedrosis virus. J. Gen. Virol. **71:**195–201.
24. **Ishida, Y., Y. Agata, K. Shibahara, and T. Honjo.** 1992. Induced expression of PD-1, a novel member of the immunoglobulin gene superfamily, upon programmed cell death. EMBO J. **11:**3887–3895.
25. **Jarvis, D. L., D. A. Bohlmeyer, and A. Garcia.** 1993. Enhancement of polyhedrin nuclear localization during baculovirus infection. J. Virol. **66:**6903–6911.
26. **Kamito, S. G., K. Majima, and S. Maeda.** 1993. Identification and characterization of the p35 gene of *Bombyx mori* nuclear polyhedrosis virus that prevents virus-induced apoptosis. J. Virol. **67:**455–463.
27. **Koerner, T. J., J. E. Hill, A. M. Myers, and A. Tzagoloff.** 1991. High-expression vectors with multiple cloning sites for construc-

tion of *trpE* fusion genes: pATH vectors. Methods Enzymol. **194:**477–490.
28. **Kunkel, T. A., J. D. Roberts, and R. A. Zakour.** 1987. Rapid and efficient site-specific mutagenesis without phenotypic selection. Methods Enzymol. **154:**367–382.
29. **LaCount, D. J., P. A. Hershberger, M. M. Donnelly, and P. D. Friesen.** Unpublished data.
30. **Laemmli, U. K.** 1970. Cleavage of structural proteins during the assembly of the head of bacteriophage T4. Nature (London) **227:**680–685.
31. **Lee, H. H., and L. K. Miller.** 1978. Isolation of genotypic variants of *Autographa californica* nuclear polyhedrosis virus. J. Virol. **27:**754–767.
32. **Lerch, R. A., and P. D. Friesen.** 1993. The 35-kilodalton protein gene (*p35*) of *Autographa californica* nuclear polyhedrosis virus and the neomycin resistance gene provide dominant selection of recombinant baculoviruses. Nucleic Acids Res. **21:**1753–1760. (Erratum, **21:**2962.)
33. **Levine, B., Q. Huang, J. T. Isaacs, J. C. Reed, D. E. Griffin, and J. M. Hardwick.** 1993. Conversion of lytic to persistent alphavirus infection by the *bcl*-2 cellular oncogene. Nature (London) **361:** 739–742.
34. **Miller, L. K.** 1988. Baculoviruses as gene expression vectors. Annu. Rev. Microbiol. **42:**177–199.
35. **Nissen, M. S., and P. D. Friesen.** 1989. Molecular analysis of the transcriptional regulatory region of an early baculovirus gene. J. Virol. **63:**493–503.
36. **O'Reilly, D. R., L. K. Miller, and V. A. Luckow.** 1992. Baculovirus expression vectors: a laboratory manual. W. H. Freeman & Co., Salt Lake City, Utah.
37. **Pearson, G. R., J. Luka, L. Petti, J. Sample, M. Birkenbach, D. Braun, and E. Kieff.** 1987. Identification of an Epstein-Barr virus early gene encoding a second component of the restricted early antigen complex. Virology **160:**151–161.
38. **Rabizadeh, S., D. J. LaCount, P. D. Friesen, and D. E. Bredesen.** 1993. Expression of the baculovirus *p35* gene inhibits mammalian neural cell death. J. Neurochem. **61:**2318–2321.
39. **Rankin, C., B. G. Ooi, and L. K. Miller.** 1988. Eight base pairs at the transcriptional start point are the major determinant for baculovirus polyhedrin gene expression. Gene **70:**39–49.
40. **Rao, L., M. Debbas, P. Sabbatini, D. Hockenbery, S. Korsmeyer, and E. White.** 1992. The adenovirus E1A proteins induce apoptosis, which is inhibited by the E1B 19-kDa and Bcl-2 proteins. Proc. Natl. Acad. Sci. USA **89:**7742–7746.
41. **Rice, W. C., and L. K. Miller.** 1986. Baculovirus transcription in the presence of inhibitors and nonpermissive *Drosophila* cells. Virus Res. **6:**155–172.
42. **Rodems, S. M., and P. D. Friesen.** 1993. The *hr*5 transcriptional enhancer stimulates early expression from the *Autographa californica* nuclear polyhedrosis virus genome but is not required for virus replication. J. Virol. **67:**5776–5785.
43. **Rohrmann, G. F.** 1992. Baculovirus structural proteins. J. Gen. Virol. **73:**749–761.
44. **Sugimoto, A., P. D. Friesen, and J. H. Rothman.** Baculovirus *p35* prevents developmentally programmed cell death and rescues a *ced-9* mutant in the nematode *Caenorhabditis elegans*. EMBO J., in press.
45. **Vaughn, J. L., R. H. Goodwin, G. L. Thompkins, and P. McCawley.** 1977. Establishment of two insect cell lines from the insect *Spodoptera frugiperda* (Lepidoptera: Noctuidae). In Vitro **13:**213–217.
46. **Volkman, L. E., P. A. Goldsmith, R. T. Hess, and P. Faulkner.** 1984. Neutralization of budded *Autographa californica* NPV by a monoclonal antibody: identification of the target antigen. Virology **133:**354–362.
47. **Volkman, L. E., S. N. Talhouk, D. I. Oppenheimer, and C. A. Charlton.** 1992. Nuclear F-actin: a functional component of baculovirus-infected lepidopteran cells. J. Cell Sci. **103:**15–22.
48. **White, E., and R. Cipriani.** 1989. Specific disruption of intermediate filaments and the nuclear lamina by the 19-kDa product of the adenovirus E1B oncogene. Proc. Natl. Acad. Sci. USA **86:** 9886–9890.
49. **White, E., and R. Cipriani.** 1990. Role of adenovirus E1B proteins in transformation: altered organization of intermediate filaments in transformed cells that express the 19-kilodalton protein. Mol. Cell. Biol. **10:**120–130.
50. **White, E., P. Sabbatini, M. Debbas, W. S. M. Wold, D. I. Kusher, and L. R. Gooding.** 1992. The 19-kilodalton adenovirus E1B transforming protein inhibits programmed cell death and prevents cytolysis by tumor necrosis factor α. Mol. Cell. Biol. **12:**2570–2580.
51. **Whitford, M., S. Stewart, J. Kuzio, and P. Faukner.** 1989. Identification and sequence analysis of a gene encoding gp67, an abundant envelope glycoprotein of the baculovirus *Autographa californica* nuclear polyhedrosis virus. J. Virol. **63:**1393–1399.
52. **Williams, G. T., and C. A. Smith.** 1993. Molecular recognition of apoptosis: genetic controls on cell death. Cell **74:**777–779.
53. **Zhong, L., T. Sarafian, D. J. Kane, A. C. Charles, S. P. Mah, R. H. Edwards, and D. E. Bredesen.** 1993. *bcl-2* inhibits death of central neural cells induced by multiple agents. Proc. Natl. Acad. Sci. USA **90:**4533–4537.